Absorbed dose delivered by alpha particles calculated in cylindrical geometry

D. Nikezic[1], A.K.M.M. Haque, K.N. Yu*

Department of Physics and Materials Science, City University of Hong Kong, Tat Chee Avenue, Kowloon Tong, Kowloon, Hong Kong

Abstract

The present work aims to develop a semi-analytical method to calculate the absorbed dose delivered by alpha particles in a cylindrical geometry. This method will be employed to reproduce the dose conversion coefficients or absorbed fraction of alpha particles in sensitive cells of the tracheobronchial tree obtained by NRC and ICRP, respectively. The difference caused by using water stopping power and tissue stopping power will also be investigated. Linear stopping powers for alpha particles in tissue and air were calculated, and the dependences of stopping powers on the traveled distance were established. A geometry model is set up for our calculations, and two different cases have been considered, namely the near-wall and far-wall cases. The total energy imparted to a unit-diameter sphere around a point is shown to be obtainable from a triple integral, which can be solved numerically. The absorbed dose is found to be independent of the diameter of the sphere being considered and additional assumptions about its diameter were not needed. The results obtained are in good agreement with those obtained previously by NRC and ICRP66. Using the semi-analytical method developed in the present work, the dose conversion coefficients or absorbed fraction previously obtained by NRC and ICRP, respectively, have been satisfactorily reproduced. Using the tissue stopping power instead of the water stopping power can slightly lower the values for dose conversion coefficients in the bronchial region. © 2002 Elsevier Science Ltd. All rights reserved.

Keywords: Lung dosimetry model; Radon; Dose conversion coefficients

*Corresponding author. Tel.: +852-2788-7812; fax: +852-2788-7830.
  E-mail addresses: peter.yu@cityu.edu.hk (K.N. Yu).
[1] On leave from University of Kragujevac, Faculty of Science, 34000 Kragujevac, Yugoslavia.

1. Introduction

The human organ, which receives the largest inhalation dose from short-lived radon progeny, is the respiratory tract, in particular, the upper part of the tracheobronchial (T-B) tree. Calculation of the dose in sensitive sells of the T-B tree is a rather complicated task and dosimetric models are needed for such calculations (ICRP, 1994 (ICRP66); NRC, 1991). A dosimetric model consists of many sub-models such as models on the lung morphometry, deposition and clearance, etc.

One of these sub-models calculates the dose absorbed in the tissue of interest per one emitted alpha particle. This task was handled by ICRP66 using the Monte Carlo method. The results were given in absorbed fraction (AF) of alpha particles, which was the fraction of alpha energy absorbed in the tissue of interest. Moreover, ICRP66 used the stopping power for alpha particles in liquid water and air adopted from ICRU (1993) (ICRU49). It is interesting that ICRP66 did not use the stopping power data in striated tissue, which were also given in ICRU49. Details of their other calculations were not given. For example, it was not mentioned whether the dose was first calculated at a point (the problem of dose calculation at a point by Monte Carlo method is not yet solved satisfactorily (Lux & Koblinger, 1991)) and the dose was then averaged in the layer of interest, or whether the absorbed energy in a layer was calculated as the difference between the input and output energies of alpha particles in that layer.

Similar calculations were performed by NRC, but they used the theoretical stopping power of Armstrong and Chandler (1973). NRC gave results in terms of the dose conversion coefficient with the unit nGy per disintegration/cm^2.

In the present work, the absorbed dose per alpha particle was calculated using a semi-analytical method based on the work of Haque (1967). The model of the airway wall was adopted from ICRP66. The original Haque's model dealt with alpha-particle sources distributed on the mucus surface and the dose was calculated in a unit-diameter sphere. The main modification made here is to extend the alpha-particle source to be the volume of the airway wall. It will be shown that the absorbed dose from alpha particles calculated in cylindrical geometry adopted for airway tubes in the T-B tree can be expressed in an analytical form with a triple integral, and Monte Carlo methods are not needed. The integration can be carried out numerically. It will also be shown that the unit-diameter sphere is no longer required. Furthermore, calculations are performed for stopping powers of alpha particles in both striated tissue and liquid water to examine their possible effects on the dose conversion coefficient.

2. Methodology

2.1. Stopping powers

The concept of "tissue equivalent path length of alpha particle" introduced by Haque (1967) was employed. Alpha particles can pass through the air cavity in an

airway tube. Our Monte Carlo calculations revealed that 46–48% of the alpha particles emitted in the mucus passed through the air cavity of a bronchus. The path length of an alpha particle in air was multiplied with the ratio, $T_{air/tissue}$, between the stopping power in air and in tissue, to give the tissue equivalent path length for those alpha particles passing through air. The mass stopping powers for striated tissue, air and water are given in Table 1. Linear stopping powers for alpha particles in tissue were recalculated from the data in Table 1 using the tissue density 1.045 g/cm^3, and those in air obtained using the air density 0.001293 g/cm^3. The ratios between the air and tissue linear stopping powers are also given in Table 1 and Fig. 1 (lower curve). Changes in the ratio with alpha energy were insignificant and were neglected, and the value $T_{air/tissue} = 0.00107$ was used in our calculations (cf. the value $T_{air/tissue} = 0.00092$ used by Haque, 1967). The upper curve in Fig. 1 represents the ratio between the stopping powers in air and in water, and the value $T_{air/water} = 0.00112$ is used as the average in our calculations.

In Table 1, stopping powers $S(E)$ of alpha particles in tissue as well as in other media are given as a function of alpha energy E. To establish the dependence of S on the traveled distance l, i.e., $S(l)$, the following procedures are followed. First, the linear stopping powers of alpha particles in the tissue were fitted by the function:

$$-\frac{\mathrm{d}E}{\mathrm{d}x} = S(E) = \sum_{i=1}^{5} a_i E^{b_i} e^{c_i E} \tag{1}$$

which gave the coefficients:

$$
\begin{aligned}
a1 &= 100.5155; & b1 &= -0.1528; & c1 &= -0.1783, \\
a2 &= 418.1634; & b2 &= 0.6306; & c2 &= -0.1233, \\
a3 &= 1813.9154; & b3 &= 0.6750; & c3 &= -0.6060, \\
a4 &= 4053.5490; & b4 &= 2.2171; & c4 &= -2.8461, \\
a5 &= 3398.0426; & b5 &= 0.6641; & c5 &= -1.6707.
\end{aligned}
$$

The fit was better than 1% in the region of interest ($E < 7.69$ MeV). The stopping powers of alpha particles in water were also fitted by Eq. (1) giving the following coefficients:

$$
\begin{aligned}
a1 &= 87.9158; & b1 &= -0.1665; & c1 &= -0.4934, \\
a2 &= 364.3784; & b2 &= 0.6120; & c2 &= -0.1102, \\
a3 &= 1352.2062; & b3 &= 0.6539; & c3 &= -0.5076, \\
a4 &= 3938.6284; & b4 &= 2.6038; & c4 &= -3.6492, \\
a5 &= 3499.2944; & b5 &= 0.6731; & c5 &= -1.3646.
\end{aligned}
$$

The energy of an alpha particle after traversing a distance x in the tissue can be determined as follows. From Eq. (1),

$$-\frac{\mathrm{d}E}{S(E)} = \mathrm{d}x \tag{2}$$

Table 1
Stopping power of alpha particles in striated tissue adopted from ICRU (1993) (ICRU49) and used in this work

Energy (MeV)	Tissue (MeV cm^2/g)	Air (MeV cm^2/g)	Water (MeV cm^2/g)	Ratio of linear stopping powers (air/tissue)
0.001	327.3	221.5	327.1	8.373E-04
0.0015	332.4	234.2	330.5	8.717E-04
0.002	337.2	244.4	334.2	8.968E-04
0.0025	342.6	253.6	338.6	9.158E-04
0.003	348.4	262.2	343.5	9.311E-04
0.004	360.9	278.4	354.6	9.544E-04
0.005	374.1	293.7	366.7	9.714E-04
0.006	387.7	308.4	379.3	9.842E-04
0.007	401.3	322.5	392.1	9.943E-04
0.008	415	336.2	404.9	1.002E-03
0.009	428.5	349.5	417.7	1.009E-03
0.01	441.9	362.5	430.4	1.081E-03
0.0125	474.5	393.3	461.5	1.025E-03
0.015	505.8	422.5	491.6	1.033E-03
0.0175	535.8	450.1	520.5	1.039E-03
0.02	564.7	476.5	548.4	1.044E-03
0.0225	592.6	501.8	575.2	1.047E-03
0.025	619.4	526	601.2	1.050E-03
0.0275	645.4	549.4	626.3	1.053E-03
0.03	670.5	572	626.3	1.055E-03
0.035	718.5	615	691.7	1.059E-03
0.04	763.9	655.7	741.1	1.062E-03
0.045	807.1	694.2	783	1.064E-03
0.05	848.2	731	823	1.066E-03
0.055	887.7	766.1	861.2	1.067E-03
0.06	925.5	799.8	898	1.069E-03
0.065	961.9	832.3	933.3	1.070E-03
0.07	997	863.6	967.4	1.071E-03
0.075	1031	893.8	1000	1.072E-03
0.08	1064	923	1032	1.073E-03
0.085	1096	951.4	1063	1.074E-03
0.09	1126	978.8	1093	1.075E-03
0.095	1156	1006	1122	1.076E-03
0.1	1185	1031	1151	1.076E-03
0.125	1320	1151	1281	1.078E-03
0.15	1439	1257	1397	1.080E-03
0.175	1544	1352	1500	1.083E-03
0.2	1640	1437	1593	1.084E-03
0.225	1725	1513	1677	1.085E-03
0.25	1802	1582	1752	1.086E-03
0.275	1871	1643	1820	1.086E-03
0.3	1933	1698	1881	1.086E-03
0.35	2039	1792	1985	1.087E-03
0.4	2122	1866	2069	1.088E-03
0.45	2187	1923	2134	1.087E-03
0.5	2235	1964	2184	1.087E-03

Table 1 (*continued*)

Energy (MeV)	Tissue (MeV cm^2/g)	Air (MeV cm^2/g)	Water (MeV cm^2/g)	Ratio of linear stopping powers (air/tissue)
0.55	2270	1993	2220	1.086E-03
0.6	2293	2012	2245	1.085E-03
0.65	2306	2020	2260	1.083E-03
0.7	2310	2021	2266	1.082E-03
0.75	2307	2016	2266	1.081E-03
0.8	2299	2005	2260	1.079E-03
0.85	2285	1989	2248	1.077E-03
0.9	2267	1970	2233	1.075E-03
0.95	2246	1948	2215	1.073E-03
1	2223	1924	2193	1.070E-03
1.25	2065	1776	2052	1.064E-03
1.5	1896	1626	1898	1.061E-03
1.75	1744	1495	1754	1.060E-03
2	1612	1383	1625	1.061E-03
2.25	1500	1288	1521	1.062E-03
2.5	1403	1206	1415	1.063E-03
2.75	1319	1134	1333	1.063E-03
3	1246	1072	1257	1.064E-03
3.5	1123	969.3	1133	1.067E-03
4	1026	886.5	1035	1.069E-03
4.5	945.3	818.6	953.5	1.071E-03
5	877.9	761.2	885.5	1.072E-03
5.5	820.6	712.2	827.5	1.073E-03
6	771.2	670	777.7	1.074E-03
6.5	727.9	633.1	734	1.076E-03
7	689.7	600.5	695.4	1.077E-03
7.5	655.8	571.6	661.2	1.078E-03
8	625.5	545.6	630.6	1.079E-03
8.5	598.1	522.2	603	1.080E-03
9	573.3	500.9	578	1.081E-03
9.5	550.8	481.5	555.2	1.081E-03
10	530.1	463.7	534.4	1.082E-03

which gives on integration:

$$\int_{E_l}^{E_0} \frac{\mathrm{d}E}{S(E)} = \int_{E_l}^{E_0} \frac{\mathrm{d}E}{\sum_{i=1}^{5} a_1 E^{b_i} e^{-c_i E}} = \int_0^l \mathrm{d}x = l, \tag{3}$$

where E_0 is the initial energy of the alpha particle and E_l its energy after traversing the distance l in tissue. The function $E(l)$, i.e., the energy of the alpha particle after traversing the distance l in tissue, can be obtained from Eq. (3) and tabulated. The stopping power $S(E_l)$ can then be calculated from Eq. (1) and the function $S(l)$ can also be tabulated. In the above calculation of $S(l)$, the step of the traversed distance for each computation was chosen to be less than 0.2 μm. These functions for alpha energies 6 and 7.69 MeV are shown in Fig. 2.
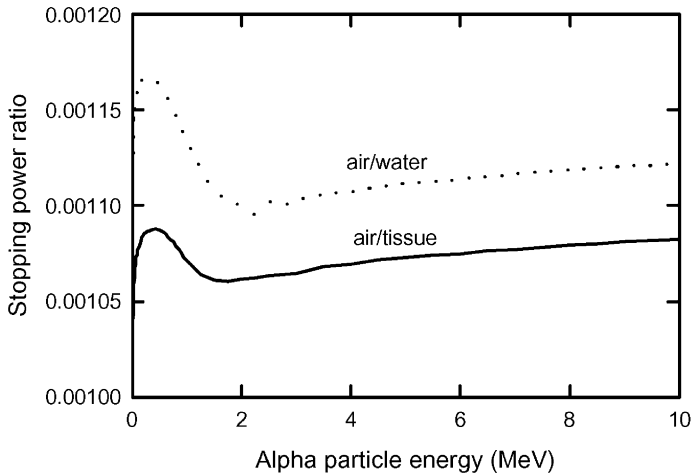
Fig. 1. Relationship between the linear stopping power ratio and the alpha-particle energy.
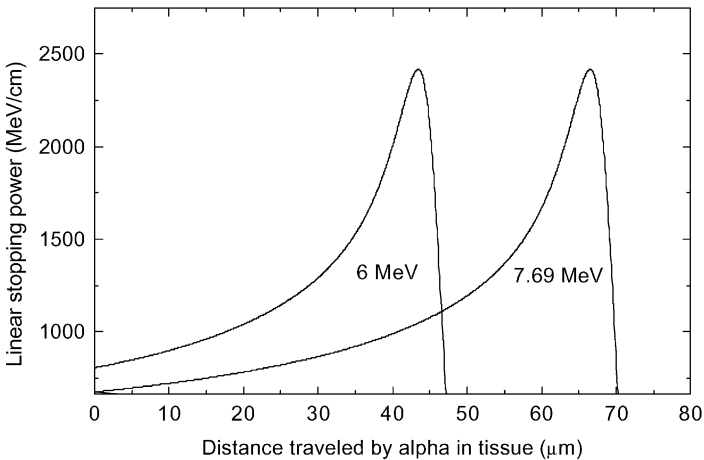

Fig. 2. Stopping power of alpha particles in tissue as a function of traveled distance for the initial alpha-particle energies of 6 and 7.69 MeV.

2.2. Geometry

The geometry model used in our calculations is shown in Fig. 3. The airway path is represented by a cylindrical tube with an inner radius r. The dose is calculated at point A at a depth a in the tissue, where the distance is measured from the inner surface of the tube, i.e., from the top of the mucus. Radioactivity is distributed between the two cylinders with radii R_1 and R_2. A tangent t is drawn from the point A on the circle with radius r, and the intersections between tangent t and circles R_1
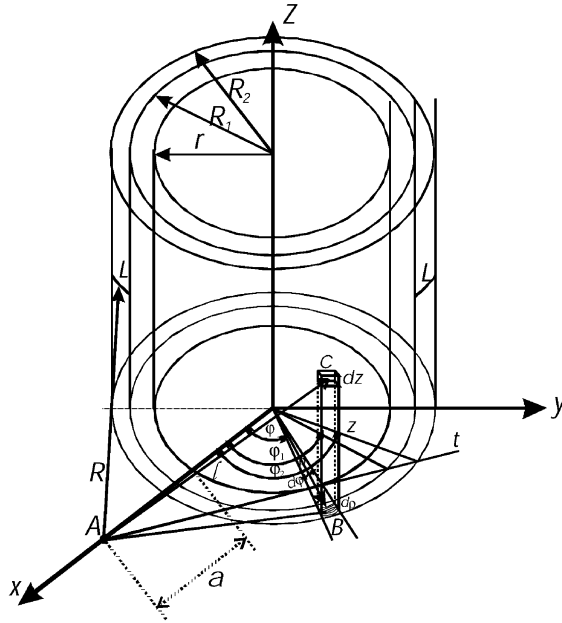
Fig. 3. Geometry considered in the present work. The airway tube is represented by a cylinder with an inner radius r. The dose is calculated at point A at the depth a of the tissue. The radioactivity is distributed between the cylinders with radii R_1 and R_2. The tangent t determines the far-wall and near-wall conditions. L is the intersection between the sphere with radius R and a cylinder.

and R_2 determine the angles φ_1 and φ_2. All the cylinders in Fig. 3 have the same axis, chosen as the z-axis. The energy imparted to the small sphere with diameter d_{sp} around A, indicated as the black circle around A, is calculated. This is firstly calculated from an infinitesimally small volume around point C that is determined in the cylindrical coordinate system with coordinates ρ, φ and z; point B is the projection of point C onto the xOy plane. R is the alpha-particle range in the tissue. The line L is obtained as an intersection between the sphere with A as center and R as radius, and the cylinder with radius R_2.

The activity dA in a small volume element around C is given by

$$dA = N\rho \, d\rho \, d\varphi \, dz, \tag{4}$$

where N is the volume specific activity, which is assumed here to be $1 \, \text{Bq}/\mu\text{m}^3$. Two different cases can be considered here, namely the near-wall and far-wall cases. The tangent t determines the near-wall cases in which the emitted alpha particles do not pass through the air cavity and their ranges are completely in the tissue. Particles emitted from the far wall traverse the air cavity and their paths are partially in air and partially in tissue.

2.2.1. Near wall

The alpha-particle flux $d\Phi$ at point A, from the source in an elementary volume C, is given as

$$d\Phi = \frac{dA}{4\pi AC^2} = \frac{N\rho \, d\rho \, d\varphi \, dz}{4\pi AC^2}.$$

(5)

The distance AC is calculated by the expression:

$$AC^2 = z^2 + (a+r)^2 + \rho^2 - 2(a+r)\rho \cos\varphi.$$

(6)

2.2.2. Far wall

In this case, the alpha-particle path is partially in air, the length of which should be replaced by the tissue equivalent path length. The geometry considered for far wall is presented in Fig. 4, where the projection onto the xOy plane is given. The new features here are the points D and X; DX is the projection of the particle path in air onto the xOy plane. The relevant distances are given by

$$AX = \frac{(d+2a)\cos\varphi - \sqrt{d^2 - (d+2a)^2\sin^2\varphi}}{2},$$

(7)

$$AB = \frac{(d+2a)\cos\varphi + \sqrt{4\rho^2 - (d+2a)^2\sin^2\varphi}}{2},$$

(8)

where $d = 2r$ is the tube diameter. AD is similarly calculated by Eq. (7), except that a positive sign replaces the negative sign before the square root. The distance AC is calculated as $AC^2 = z^2 + AB^2$. The total tissue equivalent distance AC_{tissue_eqv} for the particles traveled across the air cavity from C to A is then found as

$$AC^2_{tissue\_eqv} = z^2 + (AX + T \times DX + BD)^2,$$
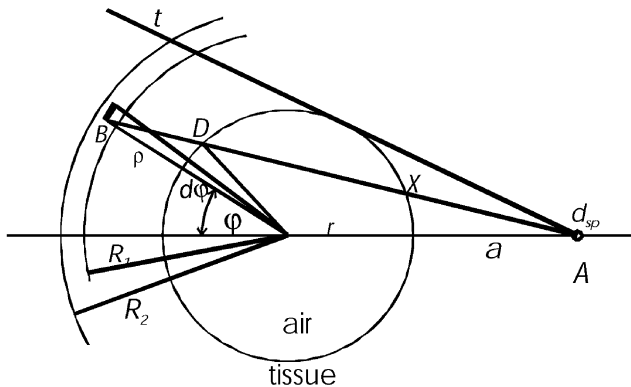
(9)

where T is the stopping power ratio defined above.

Fig. 4. Projection of the considered geometry onto the xOy plane. DX is the projection of the alpha-particle path through air. φ and ρ are variables of our integration.

2.3. Calculation of the imparted energy

The energy d^3E imparted to the small sphere with diameter d_{sp} around point A from alpha particles emitted at point C is given as a product of the particle flux, which is defined as the number of particles passing through the unit normal surface in a unit time, and stopping power of alpha particles at that point:

$$d^3E = \frac{\pi}{4}d_{sp}^2 \cdot \frac{2}{3}d_{sp} \cdot d^3\Phi \cdot S(AC_{tissue\_eqv}), \tag{10}$$

where, $\pi d_{sp}^2/4$ is the cross-sectional area of the sphere, and $2d_{sp}/3$ is the average path length of particles through the sphere of diameter d_{sp}, the former being used to determine the actual number of alpha particles that pass through the sphere.

The total energy imparted to the unit-diameter sphere around point A can be found as a triple integral in the following way:

$$\varepsilon = \frac{E}{N} = \frac{\pi}{4}d_{sp}^2\frac{2}{3}\int_{-L}^{L}\int_{R_1}^{R_2}\int_{0}^{2\pi}\frac{\rho\,d\rho\,d\varphi\,dz}{4\pi AC^2}S(AC_{tissue\_eqv}). \tag{11}$$

The energy imparted per unit volume and activity, ε, obtained from the above equation is expressed in units of $\mathrm{MeV\,s^{-1}}$. This quantity can be considered equivalent to the imparted energy per one emitted alpha particle in $1\,\mu m^3$. The integrals in the above expression cannot be solved analytically and numerical procedures should be applied. A computer program was developed to solve the integrals in Eq. (11). The variables ρ, φ and z were varied between the limits shown in Eq. (11) with the following steps: $\Delta\varphi = 0.001$ degrees for near wall and $\Delta\varphi = 1$ degree for far wall; $\Delta z = 1\,\mu m$ and $\Delta\rho = 1\,\mu m$. The energy imparted to the sphere with diameter d_{sp} should be transformed to the absorbed dose by dividing the imparted energy with the mass of the sphere which is proportional to d_{sp}^3. Therefore, the absorbed dose is independent of the sphere diameter and additional assumptions about its diameter were not needed.

3. Results and discussion

Calculations have been performed for the bronchial region or BB in ICRP66 notation, and the bronchiolar region or bb in ICRP66 notation. The average caliber of airway tube was taken as 5 mm in BB and 1 mm in bb as proposed by ICRP66. The mucus thickness was 5 μm in BB and 2 μm in bb. The depth of the tissue was calculated from the top of the mucus.

The results are given in Fig. 5 where the dependence of the dose conversion coefficient on the depth in tissue is shown. There are two pairs of curves in Fig. 5, one pair for 6 MeV, and the other for 7.69 MeV alpha-particle energy. The curves for BB and bb are very close to each other for the same alpha-particle energy, which means that the airway tube has very small influence on the dose. The curve for 7.69 MeV is above that for 6 MeV for almost all depths except in the very shallow region where the depth is smaller than 10 μm.

Calculation of the dose conversion coefficients for secretory and basal cells, which are considered sensitive to radiation, from the curves in Fig. 5 require weightings according to the mass of sensitive tissues at the given depth. In BB, secretory cells extend from 21 μm up to 51 μm, while basal cells extend from 46 up to 61 μm below the top of the mucus. In bb, secretory cells extend from 10 to 18 μm and there are no basal cells. Dose weighting from the curves in Fig. 5 has been carried out within these limits, and the dose conversion coefficients for secretory and basal cells are then obtained. The results are given in Table 2. The column labeled "water" in Table 2 was obtained using stopping power for liquid water, and the column labeled "tissue" was obtained employing data for stopping power for striated tissue (both adopted from ICRU49). For easy comparison, data from NRC are also shown in Table 2.

Agreement between the NRC data and our results are satisfactory. The only difference that may be considered significant refers to the dose delivered by 6 MeV alpha particles in basal cells. Basal cells in BB lie deep in the tissue epithelium; the basal-cell layer begins from 46 μm below the top of the mucus, which is almost at the end of the curve for 6 MeV alpha energy in Fig. 5. In other words, a relatively small
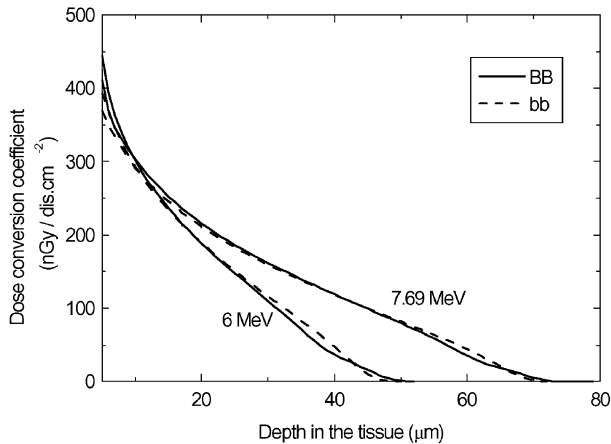

Fig. 5. Depth dose distribution for bronchi and bronchiolar region.

Table 2
Dose conversion coefficients for BB (in nGy per disintegration/cm^2)

Energy (MeV)	Secretory cells				Basal cells			
	The present work			NRC (1991)	The present work			NRC (1991)
	Water	Tissue	Differ.%		Water	Tissue	Differ.%	
6	77.2	73.2	+ 5.4	78	3.5	1.8	+ 94	3
7.69	138.1	137.8	+ 0.2	142	69.6	64.3	+ 8.2	68

number of alpha particles with an initial energy of 6 MeV can reach the basal cells. Therefore, the computed dose in basal cells hardly depends on the stopping power and the range of alpha particles used in the calculations. This also explains the large difference between the results obtained for water-and tissue-stopping power. The linear stopping power in tissue is slightly larger than that in water, so the alpha-particle range is smaller in tissue than in water. Since basal cells are close to the end of the alpha-particle range, a significantly smaller number of alpha particles would reach the basal-cell layer in tissue than in water and the dose is smaller by a factor of 2, viz. 3.5 compared to 1.8. However, the issue is not particularly important since the dose in basal cells is very small when compared to that in secretory cells and its contribution to the total dose delivered in BB is relatively small.

Table 3 shows the results for bb and good agreement between NRC data and our results are again observed.

From Table 2, the data obtained using the tissue stopping power are smaller than those obtained employing water stopping power. The discrepancies, given in the column labeled "*Differ.*" in Table 2, are different for various cases and amount up to 8% if we neglect the case for basal cells where the difference is about 95%. ICRP66 used the stopping power for liquid water and this can lead to a dose in BB a few percent larger than it should be. In bb the situation is opposite; the difference is rather small and amounts to about 1% and can be neglected.

Similar comparisons have been carried out with ICRP66 results. For this purpose, the dose conversion coefficient had to be recalculated as absorbed fraction of one alpha particle (quantity used by ICRP66). Tables 4 and 5 give the absorbed fractions

Table 3
Dose conversion coefficients for bb (in nGy per disintegration/cm^2)

Energy (MeV)	Secretory cells			NRC (1991)
	This work			
	Water	Tissue	Differ.%	
6	243.0	246.7	− 1.5	251
7.69	250.9	255.5	− 1.8	250

Table 4
Absorbed fraction of alpha particles in sensitive cells in BB

Energy (MeV)	Secretory cells			Basal cells		
	This work		ICRP66	This work		ICRP66
	Water	Tissue		Water	Tissue	
6	0.256	0.242	0.249	0.00577	0.00299	0.00506
7.69	0.356	0.357	0.353	0.09	0.08359	0.089

Table 5
Absorbed fraction of alpha particles in sensitive cells in bb

Energy (MeV)	Secretory cells		
	This work		ICRP66
	Water	Tissue	
6	0.218	0.22056	0.214
7.69	0.175	0.178	0.172

obtained in this work and those given in ICRP66. Agreement is again rather good, except in the case of basal cells where the stopping power in tissue is used.

4. Conclusions

Dose conversion coefficients or absorbed fraction of alpha particles in sensitive cells of the tracheobronchial tree have been obtained by NRC and ICRP, respectively. These have been successfully reproduced using a semi-analytical method developed and presented in the present work. This work can be considered as an independent check of NRC and ICRP66 calculations of these quantities.

The difference caused by using water stopping power and tissue stopping power in calculating the dose conversion coefficient and absorbed fraction has been examined. Using tissue stopping power instead of the water stopping power can slightly lower the values for dose conversion coefficients in BB.

References

Armstrong, T. W., Chandler, K. C. (1973). *SPAR, a FORTRAN Program for computing stopping powers and ranges of muons, charged pions, protons and heavy ions*. ORNL-4869. Oak Ridge National Laboratory, Oak Ridge, TN.

Haque, A. K. M. M. (1967). Energy expended by alpha particles in lung tissue II. A computer method of calculation. *British Journal of Applied Physics*, *18*, 657–662.

International Commission of Radiation Units and Measurements (ICRU) (1993). *Stopping powers and ranges for protons and alpha particles*. ICRU Report 49, Maryland.

International Commission on Radiological Protection (ICRP) (1994). *Human respiratory tract model for radiological protection*. ICRP66, Vol. 24 (1–3) Oxford: Pergamon Press.

Lux, I., & Koblinger, L. (1991). *Monte Carlo particle transport methods: neutron and photon calculations*. Boca Raton FL: CRC Press.

National Research Council (NRC) (1991). Comparative dosimetry of radon in mines and homes. Panel on dosimetric assumption affecting the application of radon risk estimates. NRC, National Academy Press, Washington, DC.